MINISTRY OF EDUCATION AND TRAINING

VIETNAM ACADEMY OF SIENCE AND TECHNOLOGY

GRADUATE UNIVERSITY OF SIENCE AND TECHNOLOGY

HO SY PHUONG

DEVELOPMENT OF FAULT OBSERVERS AND FAULT-TOLERANT CONTROLLERS FOR NONHOLONOMIC WHEELED MOBILE ROBOTS

SUMMARY OF DISSERTATION ON CONTROL AND AUTOMATION ENGINEERING

Code: 9 52 02 16

Ha noi - 2026

The dissertation is completed at: Graduate University of Science and Technology, Vietnam Academy of Science and Technology

Supervisor:

Supervisor 1: Dr. Ngo Manh Tien, Institute of Physics

Supervisor 2: Dr. Ngo Duy Tan, Vietnam Space Center

Referee 1:

Referee 2:

The dissertation will be examined by Examination Board of Graduate University of Science and Technology, Vietnam Academy of Science and Technology at……………………….. (time, date, year…)

This dissertation can be found at:

1) Graduate University of Science and Technology Library
2) National Library of Vietnam.

INTRODUCTION

1. Motivation

Nonholonomic wheeled mobile robots (NWMRs) are widely used in transportation, manufacturing, logistics, agriculture, healthcare, and defense. However, their nonlinear dynamics and nonholonomic constraints make accurate trajectory tracking difficult in the presence of actuator faults, disturbances, and model uncertainties.

Actuator faults may cause velocity errors, degraded tracking performance, instability, or system failure. Existing fault observers and fault-tolerant controllers still face limitations in convergence, transient response, and fault compensation. Therefore, this dissertation develops observer-based fault-tolerant control methods to improve the reliability and tracking performance of NWMRs.

Motivated by these considerations, the dissertation is entitled: "*Development of fault observers and fault-tolerant controllers for nonholonomic mobile robots*".

2. Research objectives

The dissertation aims to develop fault-tolerant control methods that ensure stable and accurate trajectory tracking under actuator faults, disturbances, and model uncertainties. The main objectives are to: Model the effects of actuator faults on NWMR dynamics and tracking errors. Develop state and fault observers. Design nonlinear observer-based fault-tolerant controllers. Improve fault compensation and tracking performance.

3. Research contents

The main research tasks are: Developing NWMR models with actuator faults and unknown disturbances. Analyzing fault effects on robot velocities and tracking errors. Improving nonlinear observers for state and fault estimation. Designing fault-tolerant controllers using estimated fault information. Evaluating the proposed methods through MATLAB/Simulink simulations.

The study focuses on two-wheel-drive NWMRs with actuator faults. Sensor faults, communication faults, obstacle avoidance, and navigation in complex environments are not considered.

4. Research methodology

The dissertation combines theoretical analysis, algorithm design, and numerical simulation. Mathematical models are established, observers and controllers are designed using nonlinear control techniques, and system stability is analyzed through Lyapunov theory. The proposed methods are then evaluated under different actuator-fault scenarios in MATLAB/Simulink.

5. Scientific and practical significance of the dissertation

The dissertation: Develops extended NWMR models including actuator faults and disturbances. Improves observer structures for state and fault estimation. Clarifies the role of integrated observer–controller architectures in fault-tolerant trajectory tracking.

The proposed methods can improve the reliability of two-wheel mobile robots, support early fault detection and compensation, and provide a basis for self-diagnosing and fault-adaptive robotic systems.

6. Novel contributions

The main contributions of the dissertation are: 1) An observer-based dual-loop fault-tolerant controller that enables effective fault estimation and compensation while ensuring stability and trajectory tracking under actuator faults. 2) A fault-tolerant control algorithm combining global integral sliding mode control, a disturbance observer, and prescribed-performance constraints.

7. Organization of the Dissertation

The dissertation consists of four chapters, an Introduction, and a General Conclusion.

Chapter 1 reviews NWMRs, trajectory-tracking control, state observation, fault estimation, and fault-tolerant control. It identifies the main research gaps in integrated observer–controller architectures.

Chapter 2 develops mathematical models and nonlinear observers for NWMRs subject to actuator faults, disturbances, and model uncertainties. The observers estimate unmeasured states, lumped disturbances, and actuator-fault effects.

Chapter 3 presents observer-based hierarchical fault-tolerant control architectures. Estimated fault and disturbance information is systematically incorporated into the control laws to improve tracking performance and robustness.

Chapter 4 develops a high-performance fault-tolerant controller combining global integral sliding mode control, a disturbance observer, and prescribed-performance constraints to regulate transient tracking behavior under actuator faults and uncertainties.

The General Conclusion summarizes the main results, discusses their scientific and practical significance, identifies remaining limitations, and suggests future research directions. The dissertation also includes the author’s related publications, references, and appendices.

CHAPTER 1. OVERVIEW OF STATE OBSERVATION, FAULT DETECTION, AND FAULT-TOLERANT CONTROL FOR NWMR

1.1 Introduction to NWMRs

Nonholonomic wheeled mobile robots (NWMRs) are autonomous systems subject to nonintegrable motion constraints and therefore cannot move instantaneously in arbitrary directions [1]. Their simple structure and high maneuverability make them widely used in transportation, logistics, inspection, and service robotics [2]. However, nonlinear dynamics, wheel–ground interaction, slip, parameter uncertainties, disturbances, and limited sensing complicate trajectory tracking [3].

Faults may occur in actuators, sensors, mechanical components, or control algorithms [4]–[6]. Actuator faults are particularly critical because they directly affect the robot's linear and angular velocities, potentially causing tracking degradation or instability [7]–[12]. Therefore, nonlinear control and observer–controller integration are essential for real-time fault detection and compensation [13]–[30].

1.2 Control methods for NWMRs

PID controllers are widely used because of their simplicity but often lose performance under nonlinearities, disturbances, wheel slip, and actuator faults [1]–[3]. Nonlinear methods, including backstepping, sliding mode control, adaptive control, and finite-time control, provide greater robustness [20]–[25].

Fault-tolerant control (FTC) is commonly classified into passive FTC and active FTC [6], [7]. Active FTC uses observers to estimate states, disturbances, and faults for online compensation [8]–[12], [51], [52]. However, reliably separating actuator faults from unknown disturbances remains challenging [11], [29].

1.3 Observation and fault-detection methods

Important variables such as wheel velocities, actuator torques, and lumped disturbances may not be directly measurable [1], [3], [30], [55]. Observers are therefore used to estimate these variables from the system model and input–output signals. Luenberger observers and Kalman filters provide the basis for linear state estimation [14], [15], [56]. Nonlinear structures, including high-gain observers, sliding mode observers, unknown-input observers, disturbance observers, and extended state observers, improve robustness under nonlinearities and uncertainties [16]–[19], [29], [57]–[59]. In model-based fault detection and diagnosis, residual signals are used to identify deviations between the nominal model and the actual system [6],

[37], [57]. Their effectiveness depends mainly on model accuracy and the ability to distinguish faults from unknown disturbances..

1.4 Observer-based fault-tolerant control

Observer–controller integration enables estimated states to be used in nonlinear feedback laws [20]–[23], [60] and allows disturbances and uncertainties to be compensated online [19], [29]. In active FTC, estimated fault information is directly incorporated into the control law [6]–[9]. Recent studies have investigated hierarchical and dual-loop architectures [13], [26], [36] and finite- or fixed-time control strategies [24], [32], [33], [41], [42]. Nevertheless, actuator faults are often included in lumped disturbances rather than estimated separately, limiting explicit diagnosis and compensation [26]–[29].

1.5 Research gaps

The literature review identifies the following gaps: Actuator faults are commonly treated as bounded disturbances or parameter uncertainties rather than explicitly estimated and compensated [7], [8], [21], [23], [40], [43], [60]. Existing active FTC methods often handle faults indirectly through extended states, lumped disturbances, or adaptive parameters [6]–[9], [12]. The integration of state, disturbance, and fault observers into an organized hierarchical kinematic–dynamic control architecture remains limited [8], [26], [36], [38], [52]. Fast convergence and prescribed transient tracking performance have rarely been addressed simultaneously under actuator faults [24], [27], [32], [51].

Accordingly, this dissertation develops observer-based FTC architectures that explicitly estimate actuator faults and systematically integrate fault compensation into hierarchical control.

1.6 Chapter 1 conclusion

This chapter reviewed trajectory-tracking control, state observation, fault detection, and FTC methods for NWMRs. Existing studies mainly improve robustness against disturbances and uncertainties, while actuator faults are usually treated indirectly. Observer integration in hierarchical control and the simultaneous assurance of fast convergence and prescribed transient performance also remain insufficiently investigated. Based on these gaps, the dissertation focuses on: An observer-based dual-loop FTC architecture for actuator-fault estimation and compensation. A fault-tolerant algorithm combining global integral sliding mode control, a disturbance observer, and prescribed-performance constraints.

CHAPTER 2. DEVELOPMENT OF ACTUATOR FAULT OBSERVERS FOR NWMRs

2.1 Mathematical model of an NWMR with actuator faults

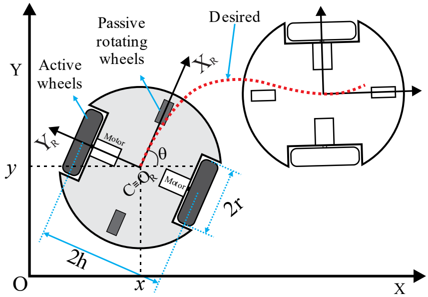

Figure 2.1. Structure of a NWMR

The robot state is defined as $q = [x, y, \theta]^T$, where x and y denote its position and θ its heading angle. The kinematic model is

$$\begin{bmatrix} \dot{x} \\ \dot{y} \\ \dot{\theta} \end{bmatrix} = \begin{bmatrix} \cos\theta & 0 \\ \sin\theta & 0 \\ 0 & 1 \end{bmatrix} \begin{bmatrix} v \\ \omega \end{bmatrix} \tag{2.3}$$

The body-frame tracking error is

$$e_q = \begin{bmatrix} x_e \\ y_e \\ \theta_e \end{bmatrix} = \begin{bmatrix} \cos\theta & \sin\theta & 0 \\ -\sin\theta & \cos\theta & 0 \\ 0 & 0 & 1 \end{bmatrix} \begin{bmatrix} x_d - x \\ y_d - y \\ \theta_d - \theta \end{bmatrix} \tag{2.4}$$

In the fault-free case, the nominal velocity command is:

$$\begin{bmatrix} v_c \\ \omega_c \end{bmatrix} = \begin{bmatrix} v_d \cos\theta_e + k_x x_e \\ \omega_d + k_y v_d y_e + k_\theta \sin\theta_e \end{bmatrix} \tag{2.6}$$

Actuator faults are represented by unknown velocity deviations:

$$\begin{cases} v_f = v - \Delta v \\ \omega_f = \omega - \Delta\omega \end{cases} \tag{2.7}$$

These faults enter the tracking-error dynamics through the same channels as the control inputs, as shown in (2.8), and are therefore treated as matched faults.

$$\dot{e}_q = \begin{bmatrix} \dot{x}_e \\ \dot{y}_e \\ \dot{\theta}_e \end{bmatrix} = \begin{bmatrix} \omega y_e - v + v_d \cos\theta_e - \Delta\omega y_e + \Delta v \\ -\omega x_e + v_d \sin\theta_e + \Delta\omega x_e \\ \omega_d - \omega + \Delta\omega \end{bmatrix} \tag{2.8}$$

The robot dynamics are derived from the DC-servo motor model and reduced to:

$$M_r(\theta)\dot{\vartheta} + C_r(\theta,\vartheta)\vartheta + D_r = B_r(\theta)\tau,\ \vartheta = [v, \omega]^T \tag{2.24}$$

After normalization,

$$\begin{cases} \dot{v} = k_1 u_1 + k_2 v + D_1 \\ \dot{\omega} = k_3 u_2 + k_4 \omega + D_2 \end{cases} \tag{2.26}$$

The actual motor input under actuator degradation is modeled as

$$u_i^f(t) = \alpha_i u_i(t) + \Delta u_i(t) \tag{2.27}$$

where $\alpha_i \in (0,1]$ denotes the loss-of-effectiveness factor. The faulty dynamics are expressed by (2.29) and rewritten as

$$\begin{cases} \dot{v} = k_1 u_1 + k_2 v + D_v \\ \dot{\omega} = k_3 u_2 + k_4 \omega + D_\omega \end{cases} \tag{2.30}$$

where D_v and D_ω include actuator faults, model uncertainties, and external disturbances. These terms and their derivatives are assumed bounded:

$$|D_v| \le \zeta_v, |D_\omega| \le \zeta_\omega \tag{2.31}$$

$$|\dot{D}_v| \le \bar{\zeta}_1, |\dot{D}_\omega| \le \bar{\zeta}_2 \tag{2.32}$$

2.2. State and actuator-fault observer design

2.2.1. Actuator fault observer

Based on [19], the tracking-error model is written as

$$\begin{cases} \dot{z} = f(z) + g_1(z)u + g_2(z)F_a \\ e_q = z \end{cases} \tag{2.34}$$

$$\dot{z} = \begin{bmatrix} \dot{x}_e \\ \dot{y}_e \\ \dot{\theta}_e \end{bmatrix}, u = \begin{bmatrix} v_d \cos\theta_e - v \\ \omega_d - \omega \end{bmatrix}, f(z) = \begin{bmatrix} y_e \omega_d \\ v_d \sin\theta_e - x_e \omega_d \\ 0 \end{bmatrix}$$

$$g_1(z) = g_2(z) = \begin{bmatrix} 1 & -y_e \\ 0 & x_e \\ 0 & 1 \end{bmatrix}; \mathrm{F}_a = \begin{bmatrix} \Delta v \\ \Delta\omega \end{bmatrix}$$

The fault observer is defined by (2.35):

$$\begin{cases} \dot{z} = -L(z)\left[g_1(z)u + g_2(z)(z+p(z)) + f(z)\right] \\ \hat{F}_a = z + p(z) \end{cases} \tag{2.35}$$

Assuming that F_a varies slowly, the estimation-error dynamics become

$$\dot{e}_f = -\dot{z} - \dot{p}(z) = -L(z)g_2(z)e_f \tag{2.36}$$

A suitable selection of $p(z)$ and $L(z)$ ensures asymptotic convergence of the fault-estimation error [19], [62].

2.2.2. Improved actuator fault observer

The basic observer may generate a large initial estimation peak. An improved fault observer (IFO) is therefore proposed using soft-start, warm-up, and smoothing mechanisms:

$$\begin{cases} \dot{z} & = -L(t)g_2(z)z - K(t)L(t)\left[g_2(z)p(z) + f(z) + g_1(z)u\right] \\ \hat{F}_a & = z + p(z) \end{cases} \tag{2.37}$$

The time-varying gains are

$$L(t) = (1 - e^{-t/\tau_L})L_0, K(t) = 1 - e^{-(t/T_{init})^2} \tag{2.38}$$

The estimated fault is then smoothed according to (2.39) before being used for compensation.

Theorem 2.1. Under Assumption 2.3, the estimation error of observer (2.37) is uniformly ultimately bounded. If the fault varies slowly and the scheduling functions converge to their nominal values, the estimation error converges asymptotically to zero.

2.2.3. Extended state observer

An extended state observer (ESO) is designed to estimate the robot velocities and lumped disturbances:

$$\begin{cases} \dot{\hat{v}} = k_1u_1 + k_2v + \hat{D}_v - \rho_1 fal(\hat{e}_v) \\ \dot{\hat{D}}_v = -\rho_2 fal(\hat{e}_v) \\ \dot{\hat{\omega}} = k_3u_2 + k_4\omega + \hat{D}_\omega - \rho_1 fal(\hat{e}_\omega) \\ \dot{\hat{D}}_\omega = -\rho_2 fal(\hat{e}_\omega) \end{cases} \tag{2.50}$$

The nonlinear function is defined as [36], [51], [63]

$$fal(\hat{e}_i) = \begin{cases} \dfrac{\hat{e}_i}{\gamma^{1-\alpha}} & \text{if } |\hat{e}_i| \le \gamma \\ |\hat{e}_i|^\alpha sign(\hat{e}_i) & \text{if } |\hat{e}_i| > \gamma \end{cases}, i = (v, \omega), 0 < \alpha < 1 \tag{2.51}$$

Theorem 2.2. For system (2.30) and observer (2.50), under Assumption 2.1, the velocity- and disturbance-estimation errors are uniformly ultimately bounded. If $\dot{D}_v \to 0$ and $\dot{D}_\omega \to 0$, all estimation errors converge asymptotically to zero, as stated in (2.58).

2.3. Simulation Results

a) Signal from FO and IFO

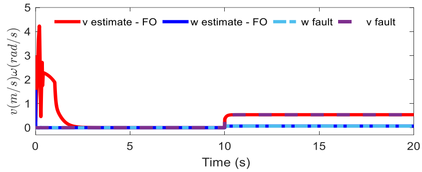

Fig. 2.3. Fault estimation from FO

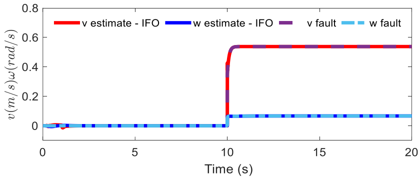

Fig.2.4. Fault estimation from IFO

b) Signal from ESO

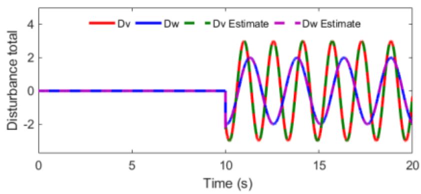

Fig. 2.5. Disturbance from ESO

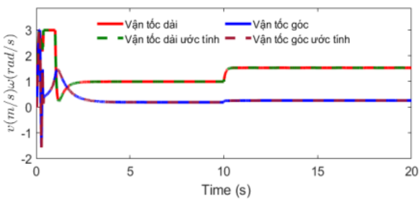

Fig. 2.6. Velocites from ESO

2.4. Chapter 2 conclusion

This chapter developed kinematic and dynamic NWMR models that explicitly account for actuator faults and lumped disturbances. A two-level observation framework combining an improved actuator fault observer and an ESO was proposed to estimate faults, velocities, and disturbances. The adaptive initialization mechanism reduces initial estimation peaks, while Lyapunov analysis establishes the boundedness and convergence of the observer errors. These results provide the basis for the observer-based fault-tolerant controllers developed in Chapter 3.

CHAPTER 3. OBSERVER-BASED HIERARCHICAL FAULT-TOLERANT CONTROL ARCHITECTURES FOR NWMRs

3.1. Fault-tolerant control based on MFC–iPID and a fault observer

3.1.1. Kinematic trajectory-tracking controller

A virtual control point $P_1(x_1, y_1)$, located at a distance Δl from the robot center, is defined as [20], [38].

$$x_1 = x + \Delta l \cos\theta, \quad y_1 = y + \Delta l \sin\theta \tag{3.1}$$

The resulting velocity commands are

$$\begin{cases} v = k_{31}e_{1x}\cos\theta + k_{32}e_{1y}\sin\theta + \dot{x}_{1d}\cos\theta + \dot{y}_{1d}\sin\theta \\ \omega = \dfrac{1}{\Delta l}\left(-k_{31}e_{1x}\sin\theta + k_{32}e_{1y}\cos\theta - \dot{x}_{1d}\sin\theta + \dot{y}_{1d}\cos\theta\right) \end{cases} \quad (3.5)$$

3.1.2. MFC–iPID dynamic controller

The uncertain robot dynamics are expressed by the ultra-local model [71], [72]:

$$\dot{\vartheta} = F_g + A_h u_{ctr} \quad (3.9)$$

where F_g represents unknown dynamics, disturbances, parameter variations, and actuator faults.

The MIMO iPID law is

$$u_{ctr} = A_h^{-1}(\dot{\vartheta}_d - \hat{F}_g + k_p e_\vartheta + k_i \int e_\vartheta dt + k_d \dot{e}_\vartheta) \quad (3.10)$$

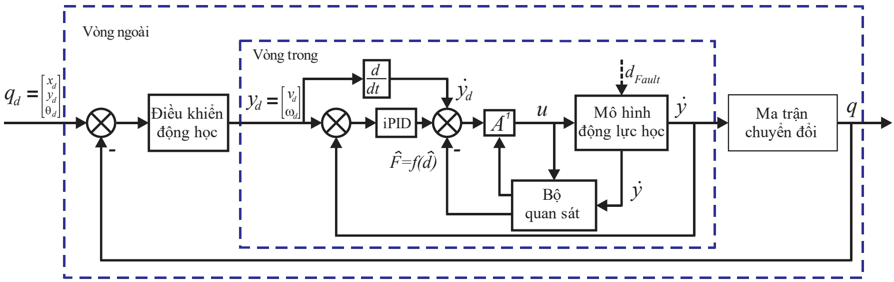

Figure 3.2. Structure of MFC-iPID

Theorem 3.1. If the estimation error $\tilde{F}_g = \hat{F}_g - F_g$ is bounded, the tracking error is uniformly ultimately bounded. If $\tilde{F}_g(t) \to 0$, the tracking error converges asymptotically to zero.

3.1.3. Simulation results

➢ *Case 1:* Conditions for no actuator errors.

Figures 3.4 and 3.5 show that the proposed controller achieves the smallest tracking error, faster response time, and superior performance compared to the other two controllers.

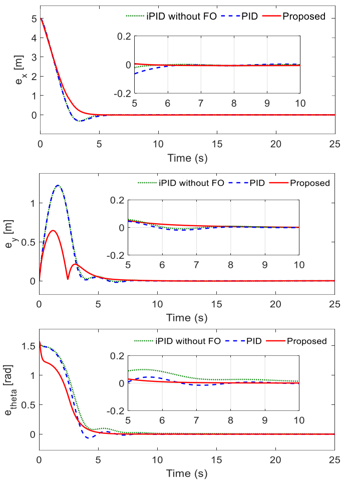

Fig. 3.4. Error tracking

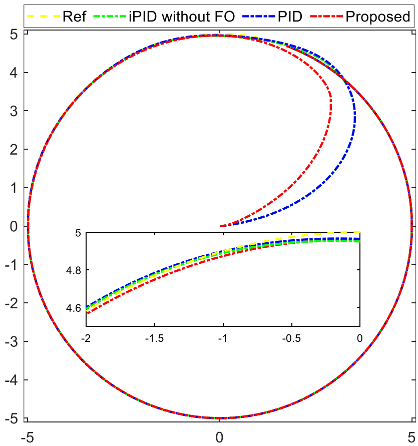

Fig. 3.5. Trajectory tracking in case 1.

➢ *Case 2:*

The proposed MFC–iPID controller was compared with conventional PID and iPID controllers. Under actuator faults introduced at $t = 8$ s, $\Delta v = 0.25v\sin(t), \Delta\omega = 0.3\omega$ with 10% variations in mass and inertia.

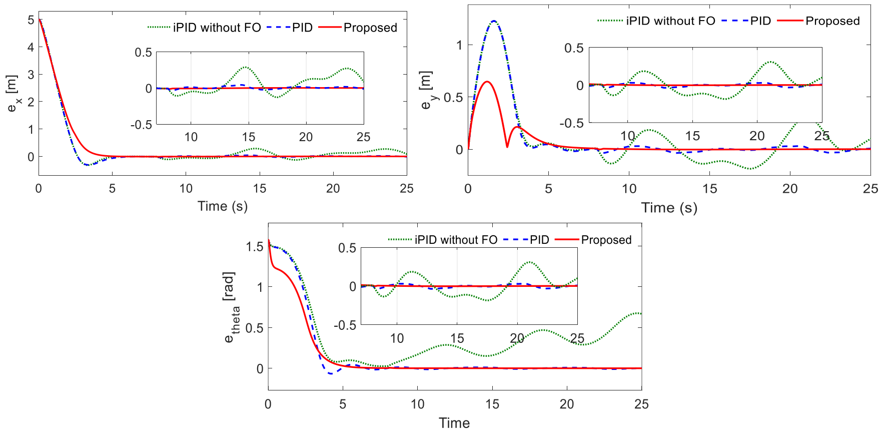

Fig. 3.6. Error tracking in case 2

The tracking error results in Figure 3.6 show that the proposed controller maintains a small deviation after the error occurs, while other controllers have larger errors. Figure 3.8 illustrates the role of the error observer. The estimated errors . $\Delta\hat{v}$ and $\Delta\widehat{\omega}$ converge quickly to the true value, with the error detection time around 8.007 s after the error is introduced into the system. This accurate estimation allows for effective error compensation in the inner control loop. Figure 3.9 confirms that the proposed controller maintains high trajectory tracking accuracy.

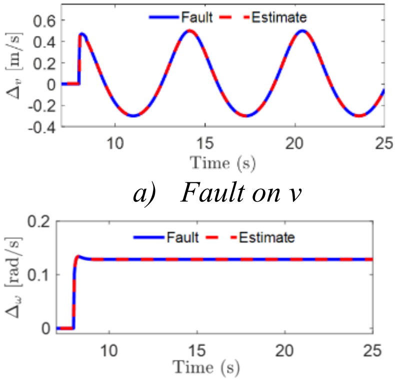

a) Fault on v

b) Fault on w

Fig. 3.8. Faults estimation

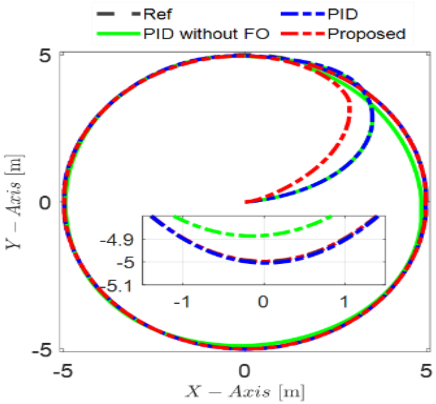

Fig. 3.9. Trajectory tracking in case 2

3.2. Dual-observer-aided sliding mode fault-tolerant control

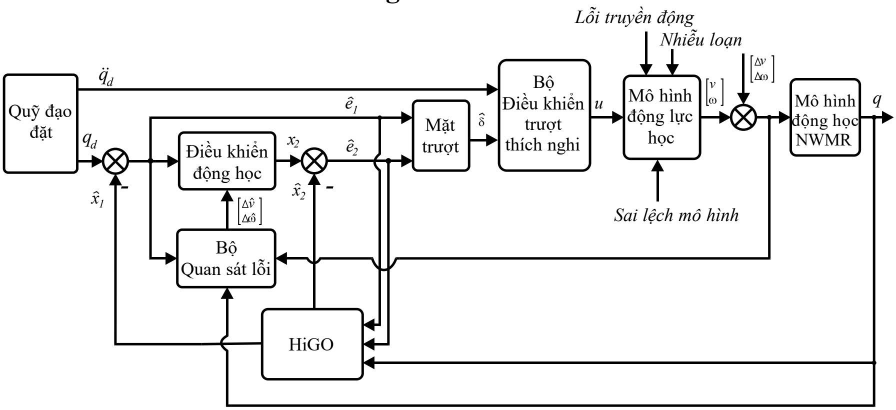

Figure 3.10. Structure of DOA-SMC.

The proposed DOA–SMC architecture combines an extended high-gain observer (HiGO), an actuator fault observer, and an adaptive sliding mode controller. HiGO estimates unmeasured velocities, while the fault observer reconstructs actuator faults.

3.2.1. Extended High-Gain Observer

Let $z_1 = [x \;\; y \;\; \theta]^T$, $z_2 = [v \;\; \omega]^T$ so that

$$\begin{cases} \dot{z}_1 = S z_2 \\ \dot{z}_2 = B\tau + D \end{cases} \tag{3.15}$$

The HiGO is designed as [16]:

$$\begin{cases} \dot{\hat{z}}_1 = S\hat{z}_2 - \dfrac{\gamma_2}{\varepsilon}\hat{e}_{z_1} \\ \dot{\hat{z}}_2 = S^{\dagger}\left(-\dfrac{\gamma_1}{\varepsilon^2}\hat{e}_{z_1}\right) \end{cases} \tag{3.16}$$

With a sufficiently small ε, the observation errors converge exponentially toward zero.

3.2.2. Adaptive Sliding Mode Controller

The fault-compensated kinematic law is

$$\begin{bmatrix} v_c \\ \omega_c \end{bmatrix} = \begin{bmatrix} v_d C\theta_e + k_x x_e + \Delta\hat{v} \\ \omega_d + k_y v_d y_e + k_\theta S\theta_e + \Delta\hat{\omega} \end{bmatrix} \tag{3.25}$$

The dynamic controller uses the observer-based sliding variable defined in (3.27) and the adaptive switching law in (3.31). The continuous $\tanh(\cdot)$function is employed to reduce chattering.

$$\begin{cases} u = B^{-1}\left(S^{-1}\ddot{q}_d - \lambda S\hat{e}_{z_2} - \hat{\lambda}_{sw}\tanh(\hat{\delta})\right) \\ \dot{\hat{\lambda}}_{kw} = \hat{\lambda}_{kw}\left|\hat{\delta}\right|\left(1 + \dfrac{2}{e_\lambda \pi}\left|atan2\left(\xi, \hat{\delta}\right)\right|\right) \end{cases} \tag{3.31}$$

Theorems 3.2–3.4 establish that the kinematic tracking errors converge to zero, while the tracking and observer errors of the complete DOA–SMC system are uniformly ultimately bounded under bounded faults and disturbances.

3.2.3. Simulation results

From 10s to 15s, the actuator output experienced a fixed performance degradation 45%, $\Delta v(t) = 0.45v, \Delta\omega(t) = 0.45\omega$; From 20s to 25s, the actuator experienced sinusoidal degradation with: $\Delta v(t) = 0.45v\, sin(t)\, , \Delta\omega(t) = 0.45\omega\cos(t + \pi/2)$; From 30s to 35s, a bias faults was introduced: $\Delta v(t) = 0.45v - 0.15, \Delta\omega(t) = 0.45\omega - 0.15$. Disturbances $Dis = [3\sin(t) \quad 2\cos(t)]^T$ affected the system from 10s to 35s. Model parameter error $m = 69.263 + 7\eta_R, I = 4.729 + 0.5\eta_R$, $0 < \eta_R < 1$.

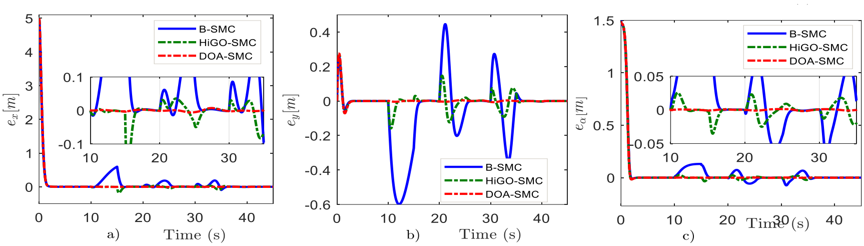

Fig. 3.11. Errors tracking: (a) x_e; (b) y_e; (c) θ_e

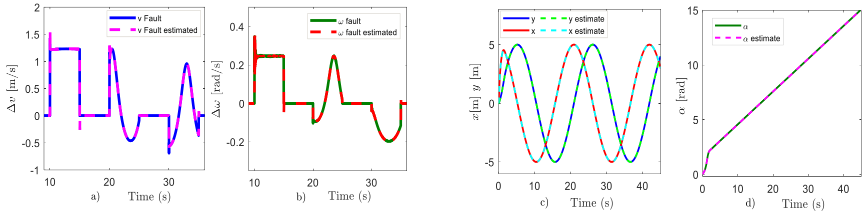

Fig. 3.13. (a) linear velocity error; (b) angular velocity error; (c) position along the X and Y axes; (d) orientation angle.

Figs 3.11–3.14 present a comparison of the performance of the three controllers under different actuator fault conditions. The results show that the DOA–SMC controller achieved the best tracking accuracy on the x, y axes and the directional angle θ. For directional control, DOA–SMC achieved RMSE = 0.2176 and IAE = 1.7231, better than B–SMC (RMSE = 0.2216, IAE = 2.7377), while HiGO–SMC showed intermediate performance but had larger transients when LoE faults occurred.

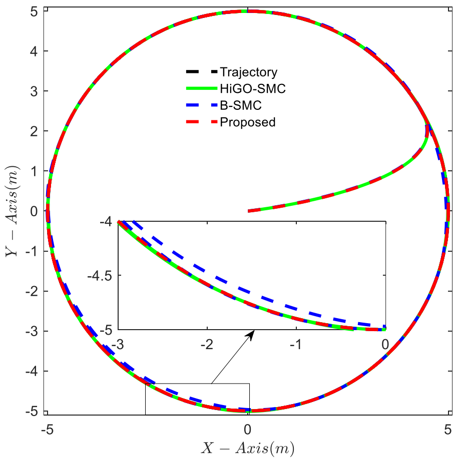

Fig. 3.14. Trajectory tracking when fault occurs

The DOA-SMC's control signal reacts quickly after an fault occurs, allowing for rapid error convergence without saturating the actuator, while maintaining the lowest possible control effort. Quantitative indicators show that DOA-SMC reduces positional RMSE by approximately 10% and IAE by up to 63.8% compared to B-SMC, demonstrating the effectiveness of the dual-observation structure in improving accuracy and fault tolerance.

Tables 3.5. – 3.6: Tracking performance index for error

Index	**DOA-SMC**		**B-SMC**		**HiGO-SMC**	
	direction	*Euclide total*	*direction*	*Euclide total*	*direction*	*Euclide total*
MSE	0. 0474	0.2134	0. 0491	0.2648	0. 0474	0.2648
MAE	0. 0383	0. 0663	0. 0608	0. 1831	0. 0423	0. 1831
RMSE	0. 2176	0. 4620	0. 2216	0. 5146	0. 2177	0. 5146
IAE	1. 7231	2. 9851	2. 7377	8. 2424	1. 9041	8. 2424
ISE	2. 1316	9. 6068	2. 2100	11. 9197	2. 1323	11. 9197

3.3. Hierarchical fault-tolerant control based on IFO and SMC–ESO

The proposed architecture separates the control task into an inner dynamic loop and an outer kinematic loop. The inner loop combines SMC with an ESO, whereas the outer loop combines fuzzy gain adaptation with the IFO.

3.3.1. Inner-loop SMC–ESO controller

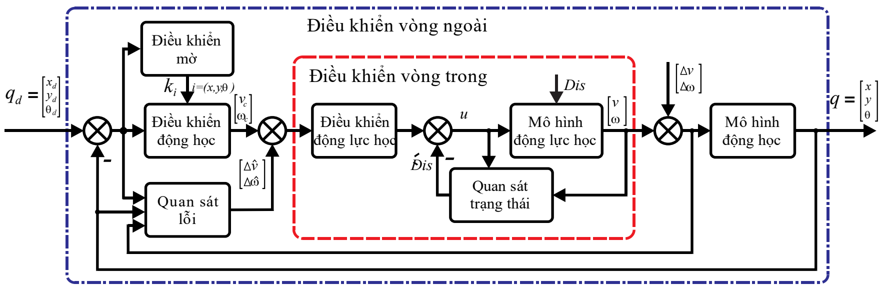

Fig. 3.15. Structure of FB-IFO-SMC-ESO

The PI sliding surface is defined as [70]:

$$\sigma = \begin{bmatrix} \sigma_1 \\ \sigma_2 \end{bmatrix} = \begin{bmatrix} e_v + k_v \int e_v dt \\ e_\omega + k_\omega \int e_\omega dt \end{bmatrix}, (k_v, k_\omega > 0) \tag{3.48}$$

The equivalent controller directly compensates for the ESO estimates $\widehat{D}_v$ and $\widehat{D}_\omega$, while a continuous switching component improves robustness:

$$u_{SMC} = u_{eq} + u_{sw} = \begin{bmatrix} \frac{1}{k_1}\left(k_v e_v + \dot{v}_{ref} - k_2 v - \hat{d}_1\right) + k_{sw1}\tanh(\sigma_1) \\ \frac{1}{k_3}\left(k_\omega e_\omega + \dot{\omega}_{ref} - k_4 \omega - \hat{d}_2\right) + k_{sw2}\tanh(\sigma_2) \end{bmatrix} \quad (3.54)$$

Theorem 3.5. Under Assumption 2.1, the SMC–PI law (3.54), together with the ESO (2.50), drives the sliding variable to zero in finite time despite bounded disturbances.

3.3.2. Outer-loop fuzzy–IFO controller

The outer-loop control law is

$$\begin{bmatrix} v \\ \omega \end{bmatrix} = \begin{bmatrix} v_d \cos\theta_e + k_x x_e + \Delta v \\ \omega_d + k_y v_r y_e + k_\theta \sin\theta_e + \Delta\omega \end{bmatrix} \quad (3.71)$$

The IFO estimates Δv and $\Delta\omega$, while a Mamdani fuzzy system adjusts k_x, k_y, and k_θ online using the tracking error and its derivative [44].

Table 3.7. Value of k_x

kx		***e***								
		NL	**NB**	**NM**	**NS**	**Z**	**PS**	**PM**	**PB**	**PL**
de	**NL**	PM	PM	PM	PM	PM	PB	PB	PB	PL
	NB	PM	PM	PM	PM	PM	PB	PB	PB	PL
	NM	PS	PM	PM	PM	PM	PM	PB	PB	PL
	NS	PS	PS	PS	PS	PS	PM	PM	PM	PB
	Z	Z	Z	Z	Z	Z	PS	PM	PM	PB
	PS	NS	NS	Z	Z	Z	PS	PS	PS	PS
	PM	NM	NM	NS	NS	NS	NS	Z	PS	PS
	PB	NL	NB	NM	NS	Z	Z	Z	PS	PS
	PL	NL	NB	NM	NS	Z	Z	Z	PS	PS

Table 3.8. Value of k_y

ky		***e***								
		NL	**NB**	**NM**	**NS**	**Z**	**PS**	**PM**	**PB**	**PL**
de	**NL**	PB	PM	PS	Z	NS	NS	NM	NB	NL
	NB	PB	PM	PM	Z	NS	NS	NM	NB	NL
	NM	PB	PM	PM	Z	NS	NS	NM	NM	NL
	NS	PL	PB	PM	PS	Z	NS	NS	NM	NB
	Z	PL	PB	PM	PS	Z	Z	NS	NS	NB
	PS	PL	PB	PM	PS	Z	Z	NS	NS	NM

	PM	PL	PB	PM	PS	Z	Z	NS	Z	PS
	PB	PL	PB	PB	PS	Z	Z	Z	Z	PS
	PL	PL	PB	PB	PS	Z	Z	Z	Z	PS

Table 3.9. Value of k_θ

k_x		*e*								
		NL	**NB**	**NM**	**NS**	**Z**	**PS**	**PM**	**PB**	**PL**
de	**NL**	PB	PM	PM	Z	NS	NS	NM	NB	NL
	NB	PB	PM	PM	Z	NS	NS	NM	NB	NL
	NM	PL	PB	PM	PS	Z	NS	NS	NM	NB
	NS	PL	PB	PM	PS	Z	Z	NS	NS	NM
	Z	PL	PB	PM	PS	Z	Z	NS	NS	NM
	PS	PL	PB	PM	PS	Z	Z	NS	Z	PS
	PM	PL	PB	PM	PS	Z	Z	NS	Z	PS
	PB	PL	PB	PB	PS	Z	Z	Z	Z	PS
	PL	PL	PB	PB	PS	Z	Z	Z	Z	PS

Theorem 3.6. For the faulty kinematic model (3.64), the controller (3.65) and IFO (2.37) ensure that the position and heading errors remain bounded and converge asymptotically to zero.

3.3.3. Simulation results

Case 1: The robot moves in a circular orbit when disturbed, no actuator faults.

$$\begin{bmatrix} D_v \\ D_\omega \end{bmatrix} = \begin{bmatrix} 6\sin(5t + pi/2) \\ 5\cos(4t + pi) \end{bmatrix} \quad (3.78)$$

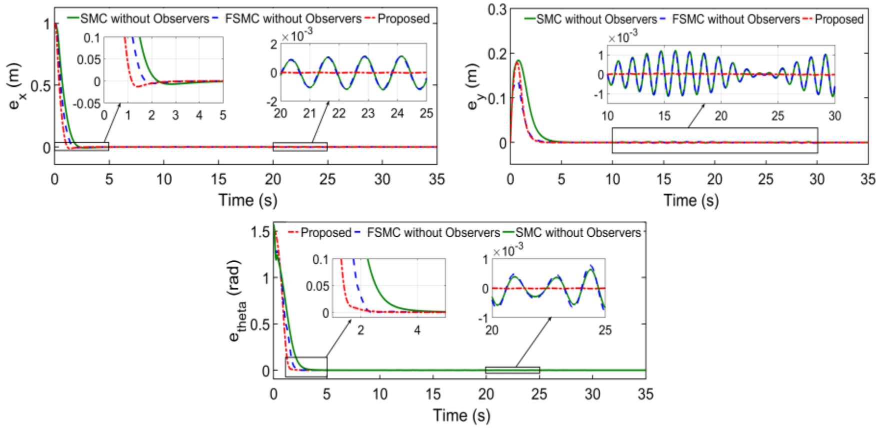

Fig. 3.19. Errors tracking (a) X-axis; (b) Y-axis; (c) theta

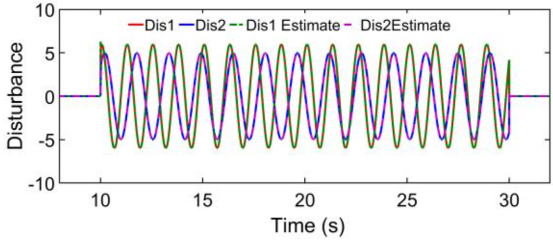

Fig. 3.21. Disturbances estimate from ESO

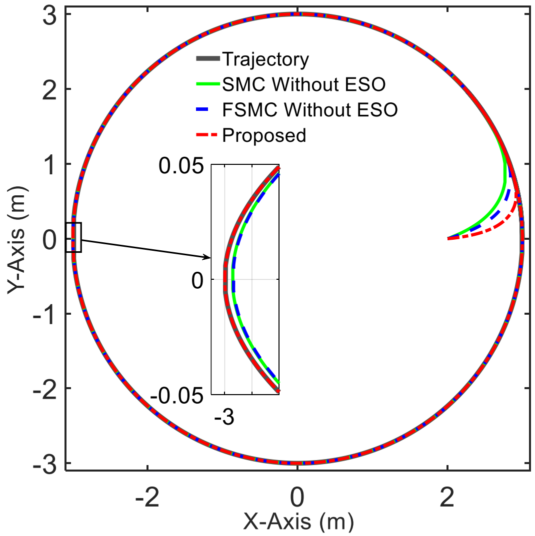

Fig. 3.22. Robot trajectories corresponding to the controllers

Figures 3.19–3.22 present the simulation results for the circular trajectory under disturbance-only conditions. Figure 3.21 shows the disturbance and its ESO estimate. The tracking errors in (x), (y), and (theta) in Figure 3.19 confirm the controller's disturbance-rejection capability, while the corresponding linear and angular velocities are shown in Figure 3.20.

Case 2. The robot moves along a figure-eight trajectory under the effects of disturbances and actuator faults.

$$\begin{bmatrix} D_v \\ D_\omega \end{bmatrix} = \begin{bmatrix} 6\sin(5t + pi/2) \\ 5\cos(4t + pi) \end{bmatrix}; \qquad \begin{bmatrix} \Delta v \\ \Delta\omega \end{bmatrix} = \begin{bmatrix} 0.3v\sin(t) \\ 0.2\omega \end{bmatrix} \tag{3.79}$$

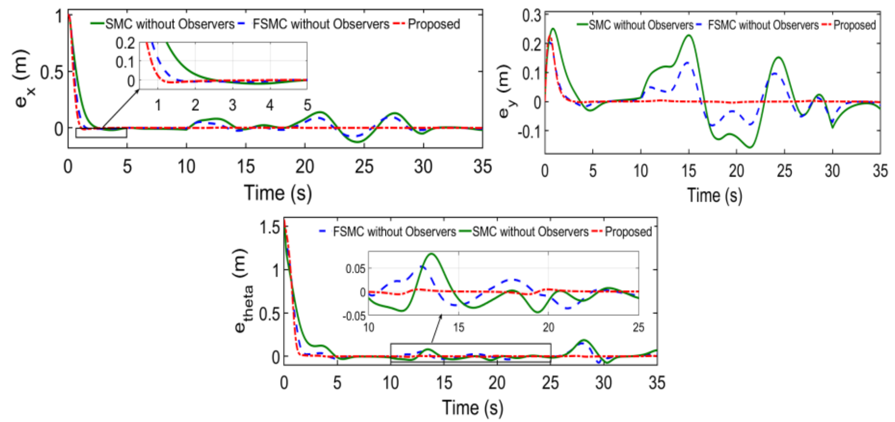

Fig. 3.24. Tracking errors for the figure-eight trajectory: (a) x-axis; (b) y-axis; (c) θ

Figures 3.24–3.26 show the robot motion along a figure-eight trajectory in the presence of both disturbances and actuator faults. With the aid of the ESO and IFO observers, the proposed controller maintains improved control performance, as reflected by faster error convergence and smoother control signals. The tracking errors in the x-axis, y-axis, and orientation angle θconverge to zero more rapidly and remain significantly smaller throughout the simulation, as shown in Figures 3.24(a)–(c). The linear and angular velocity responses in Figure 3.25 also indicate greater stability and smoother control performance of the proposed controller. Figure 3.26 presents the tracking trajectories of the three controllers. Comparing the red curve, which represents the trajectory achieved by the proposed controller, with the reference trajectory confirms the effectiveness and stability of the proposed controller.

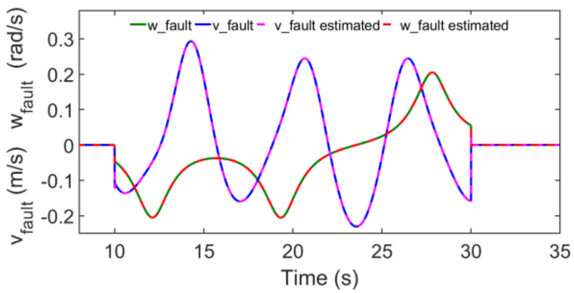

Fig. 3.23. Fault estimation using the IFO

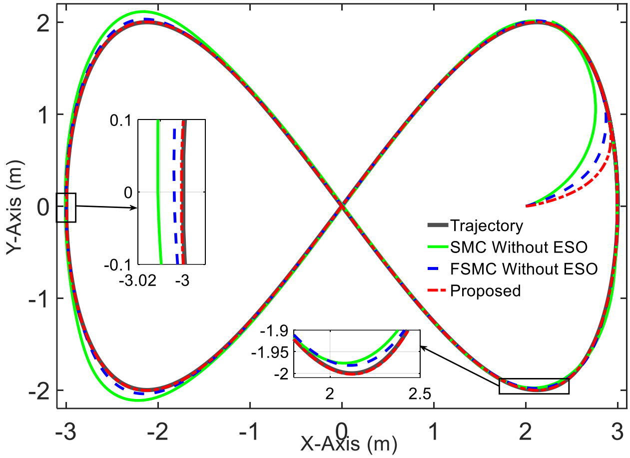

Fig. 3.26. Figure-eight trajectory tracking

3.4. Chapter 3 conclusion

This chapter developed three observer-based FTC strategies: 1) MFC–iPID with a fault observer, requiring no accurate dynamic model. 2) DOA–SMC combining HiGO and a fault observer. 3)A hierarchical architecture integrating fuzzy–IFO and SMC–ESO. The results demonstrate that systematic observer–controller integration improves fault compensation, robustness, and trajectory-tracking accuracy under actuator faults, disturbances, and model uncertainties.

CHAPTER 4. FAULT-TOLERANT CONTROL WITH PRESCRIBED-PERFORMANCE CONSTRAINTS FOR NWMRs

This chapter develops a global integral sliding mode fault-tolerant controller that combines an improved disturbance observer (IDO) with prescribed performance control. The method addresses actuator faults, wheel slip, center-of-mass offset, and model uncertainties while ensuring finite-time convergence and constrained tracking errors [67], [74].

4.1. NWMR model with actuator faults, center-of-mass offset and wheel slip

Actuator degradation changes the actual wheel velocities as [3], [10]

$$\begin{cases} \omega_R = (1-\mu_R)\omega_1 = \omega_1 - \Delta\omega_1 \\ \omega_L = (1-\mu_L)\omega_2 = \omega_2 - \Delta\omega_2 \end{cases} ; 0 < \mu_i \le 1 \tag{4.1}$$

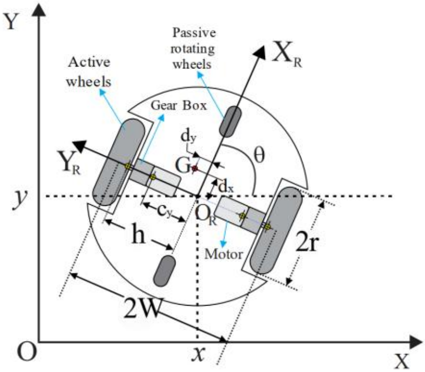

Fig. 4.1. Structure of an NWMR with an offset center of mass.

The actual robot velocities are:

$$\begin{cases} v_{real} = \dfrac{r}{2}(\omega_R + \omega_L) = v - \Delta v \\ \omega_{real} = \dfrac{r}{2h}(\omega_R - \omega_L) = \omega - \Delta\omega \end{cases} \tag{4.2}$$

With a center-of-mass offset, the kinematic model is

$$\dot{q} = S_d \vartheta,\ \vartheta = \begin{bmatrix} v & \omega \end{bmatrix}^T \tag{4.3}$$

Actuator faults, lateral and longitudinal slip, external disturbances, and parameter uncertainties are combined into a lumped disturbance. The resulting model is written as

$$\dot{z}_1 = z_2; \dot{z}_2 = N\tau + Q + z_3; \dot{z}_3 = \Delta_d \tag{4.10}$$

where z_3 represents the lumped effects of faults, slip, disturbances, and uncertainties.

The control objective is to ensure finite-time trajectory tracking within prescribed error bounds while maintaining bounded disturbance-estimation errors.

4.2. Global integral sliding mode control with an improved disturbance observer

4.2.1. Improved disturbance observer

The IDO is designed as

$$\begin{cases} \dot{\hat{z}}_1 = \hat{z}_2 + 4\xi_1 e_{z1} \\ \dot{\hat{z}}_2 = N\tau + Q + \hat{z}_3 + 4\xi_1^2 e_{z1} \\ \dot{\hat{z}}_3 = \xi_1^3 e_{z1} + \hat{\beta}_{IDO} \tanh\left(\sigma_d\right) \end{cases} \tag{4.14}$$

where $e_{z_i} = \hat{z}_i - z_i$. The adaptive gain is updated by

$$\dot{\hat{\beta}}_{IDO} = \frac{\alpha_1}{\xi_1}\psi^T P_m B_m \tanh\left(\sigma_d\right) \tag{4.19}$$

A fault alarm is generated when the estimated fault exceeds a specified threshold:

$$F_D = \begin{cases} 1 \quad \text{if} \quad \left\|\hat{F}_v\right\| > thereshold \\ 0 \quad \text{if} \quad \left\|\hat{F}_v\right\| \le thereshold \end{cases} \tag{4.22}$$

Theorem 4.1. For system (4.10), sufficiently large observer gains ξ_1 and α_1 ensure bounded observation errors.

4.2.2. GISMC with prescribed performance

The prescribed performance function is defined as [68]

$$\rho\left(t\right) = (\rho_0 - \rho_\infty)e^{-ct} + \rho_\infty \tag{4.28}$$

and the tracking error must satisfy

$$-\varsigma_d \rho\left(t\right) \; < \; e \; < \; \varsigma_u \rho\left(t\right), \; t \; > \; 0 \tag{4.29}$$

The error transformation is

$$H\left(z*\right) = \frac{\varsigma_u e^{z*} - \varsigma_d e^{-z*}}{e^{z*} + e^{-z*}} \tag{4.30}$$

$$e = \rho H\left(z*\right) \tag{4.31}$$

The global integral sliding surface is

$$\delta = \hat{z}_2 + 2\kappa_0 \varepsilon * + \kappa_0^2 \int_0^t \varepsilon * d\tau - p\left(t\right) \tag{4.33}$$

The proposed control law is

$$\tau_{GISMC} = N^\dagger \left(-Q - 2\kappa_0 \dot{z} * - \kappa_0^2 z * + \dot{p}\left(t\right) - \hat{z}_3 - \kappa_2 s - \kappa_1 \tanh\left(s\right)\right) \tag{4.36}$$

The control structure comprises three layers: prescribed-performance enforcement, lumped-disturbance estimation by the IDO, and finite-time stabilization by GISMC.

Theorem 4.2. Under Assumption 4.1, all closed-loop signals remain bounded, the sliding surface is reached in finite time, and the tracking error remains within the prescribed performance bounds.

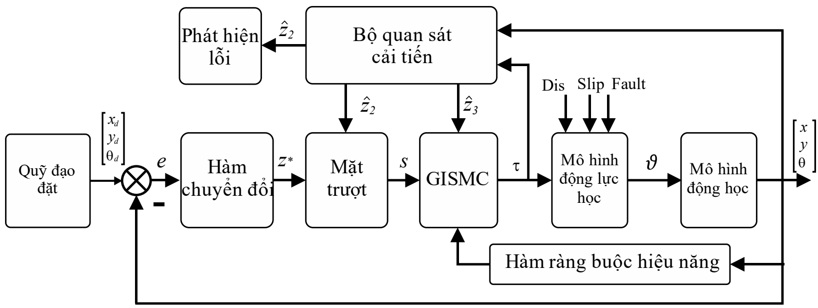

Fig. 4.2. Block diagram of the proposed controller.

4.3.2. Simulation Results

The proposed GISMC was compared with ASMC and SMC–IDO over a 45 ssimulation comprising three stages: Stage I (0s – 15s): The robot operates under nominal conditions with 10% model parameter uncertainties, i.e., ($\Delta M = 0.1M, \Delta N = 0.1N$), without external disturbances, wheel slip, or actuator faults. Stage II (15–25 s): In addition to model uncertainties, the robot is subjected to external disturbances and wheel slip, represented by $\Delta_S = [\delta_{sl} \quad -r\varpi_R \quad -r\varpi_L]^T$ where $\delta_{sl} = 5 + 0.8sin(t)$, $\varpi_R = \beta\, sin(t)$, $\varpi_L = \beta\, cos(t)$, $0 < \beta < 0.2$. Stage III (25–35 s): Actuator faults are introduced as: $\Delta v = \varepsilon v$, $\Delta \omega = \varepsilon \omega$ $(0.25 < \varepsilon < 0.35)$. Therefore, the robot is simultaneously affected by model uncertainties, external disturbances, wheel slip, and actuator faults. The robot velocities were constrained by $|\ v\ | \leq 2$ m/s, $|\ \omega\ | \leq 2.5$ rad/s.

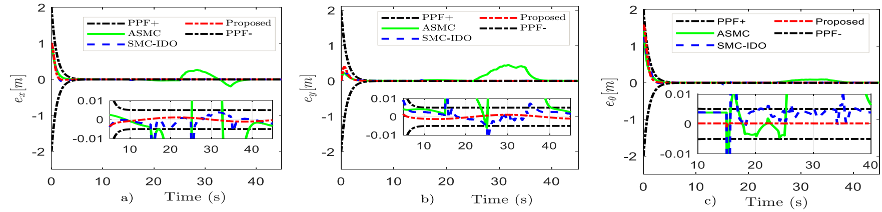

Hình. 4.3 Tracking errors along the axes X, Y and θ

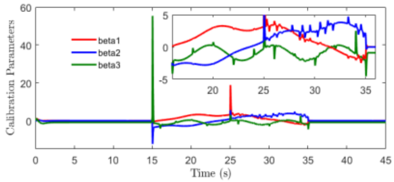

Fig. 4.4. Adaptive gain of the IDO

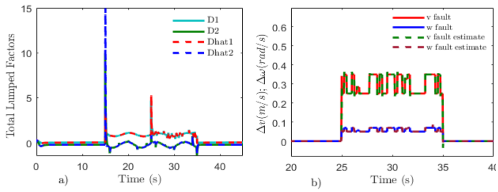

Fig. 4.5. Fault estimation and the combined effects of disturbances and wheel slip.

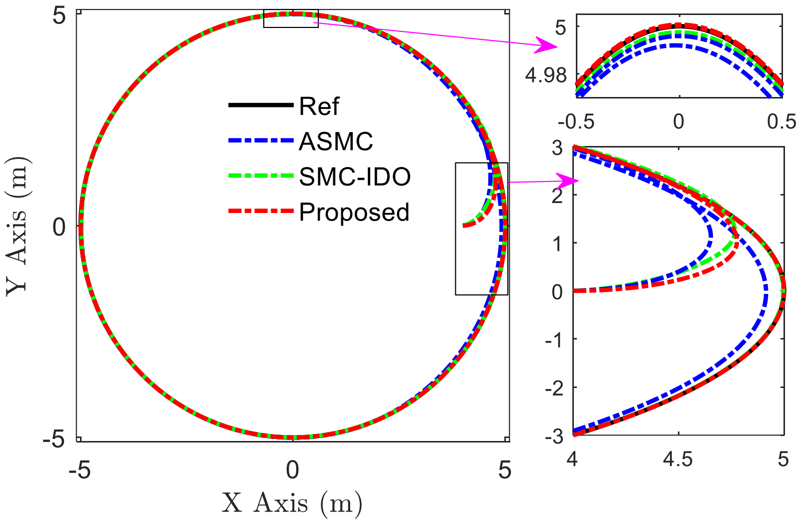

Fig. 4.8. Robot path-tracking trajectory

Table 4.3. Performance indices for the total Euclidean tracking error in the plane.

INDEX	MSE	MAE	RMSE	IAE	ISE
GISMC	0.0128	0.0217	0.1133	0.9752	0.5772
ASMC	0.0433	0.1159	0.2081	5.2156	1.9479
SMC-IDO	0.0114	0.0244	0.1067	1.0986	0.5119

GISMC achieved the lowest MAE and IAE. Compared with ASMC, both indices were reduced by approximately 81%; compared with SMC–IDO, they were reduced by approximately 11%. Although SMC–IDO produced slightly lower MSE, RMSE, and ISE, GISMC provided faster recovery, smoother control, and lower accumulated absolute error. The tracking error remained within the prescribed bounds and converged to the steady-state performance region of ±0.005m. The IDO accurately estimated the lumped disturbances and detected the actuator fault in Stage III.

4.4. Chapter 4 conclusion

This chapter proposed a high-performance fault-tolerant controller combining GISMC, an adaptive IDO, and prescribed-performance constraints. Lyapunov analysis established boundedness and finite-time convergence, while simulations confirmed robust trajectory tracking under actuator faults, wheel slip, center-of-mass offset, disturbances, and model uncertainties.

CONCLUSION

This dissertation systematically investigated fault-tolerant control for nonholonomic wheeled mobile robots (NWMRs) subject to disturbances, model uncertainties, and actuator faults. Based on the kinematic and dynamic characteristics of NWMRs, observer-based control methods were developed to improve system reliability and trajectory-tracking performance.

First, kinematic and dynamic models incorporating actuator faults, disturbances, and model uncertainties were established. An actuator-fault observation mechanism was then developed to represent faults as linear- and angular-velocity deviations, enabling their effects to be explicitly estimated and compensated at the kinematic level. Based on these estimates, observer-based fault-tolerant control strategies were designed. Their stability was established through Lyapunov analysis and verified through simulations involving disturbances, wheel slip, and actuator faults.

The dissertation provides two main scientific contributions:

1) An observer-based dual-loop fault-tolerant controller that effectively estimates and compensates for actuator faults while ensuring system stability and trajectory tracking.

2) A fault-tolerant control algorithm combining global sliding mode control, a disturbance observer, and prescribed-performance constraints.

Future work: The proposed methods will be implemented and evaluated on AGV platforms. They may also be extended to multi-robot systems to broaden the applicability of fault-tolerant control strategies for autonomous mobile robots.

DANH MỤC CÔNG TRÌNH KHOA HỌC ĐÃ CÔNG BỐ

[CT1]. H. S. Phuong, Ngo Manh Tien*, Ngo Duy Tan, Mai The Anh, Duong Dinh Tu, "*Proposal of a Fault-tolerant controller for wheeled mobile robots with faulty actuators*," 2023 12th International Conference on Control, Automation and Information Sciences (ICCAIS), Hanoi, Vietnam, pp. 507-512, 2023. DOI: 10.1109/ICCAIS59597.2023.10382286. **(SCOPUS)**

[CT2]. Sy Phuong Ho, Manh Tien Ngo*, Duy Tan Ngo, Dinh Tu Duong, Thanh Tri Nguyen, Van Vy Phan, "*Fault-Tolerant Trajectory Tracking Control for Non-holonomic Mobile Robots Using HOICD-SMC*", Advances in Engineering Research and Application. ICERA 2025. Lecture Notes in Networks and Systems, vol 1804. Springer, Cham. https://doi.org/10.1007/978-3-032-15839-0_26. **(SCOPUS-Q4)**

[CT3]. Sy Phuong Ho, Dinh Tu Duong, Van Chuong Le, Van Vy Phan, Hung Cuong Ta, Thanh Tri Nguyen, "Fault-Tolerant Control for Mobile Robots: Integrating Low-Pass Filters for Improved Actuator Fault Compensation," *2025 3rd International Conference on Smart Systems for applications in Electrical Sciences*, Tumakuru, India, 2025, pp. 1-6, doi: 10.1109/ICSSES64899.2025.11009298. **(SCOPUS-Q4)**

[CT4]. Sy Phuong Ho, Manh Tien Ngo, Duy Tan Ngo, Dinh Tu Duong, Van Chuong Le, Van Nam Dinh, Van Du Phan, "*Global Sliding Mode Fault-Tolerant Control for Non-holonomic Wheeled Robots: Ensuring Prescribed Performance in the Presence of Faults and Slippage*," in IEEE Access, vol. 14, pp. 18857-18867, 2026, doi: 10.1109/ACCESS.2026.3660656. **(SCIE-Q1)**

[CT5]. Sy Phuong Ho, Manh Tien Ngo*, Duy Tan Ngo, Dinh Tu Duong, Van Du Phan, Kim Duyen Ha Thi, Thanh Tri Nguyen, Minh Dang Dau, Thu Uyen Le Thi, "*Fault-Tolerant Trajectory Tracking of Mobile Robots via Model-Free Intelligent PID and Fault Observer"*, Bulletin of Electrical Engineering and Informatics (BEEI), vol. 15, no. 1, February 2026, pp. 184~197, DOI: 10.11591/eei.v15i1.9884 **(SCOPUS-Q3)**

[CT6]. Sy Phuong Ho, Manh Tien Ngo, Duy Tan Ngo, Dinh Tu Duong, Kim Duyen Ha Thi*, Thanh Tri Nguyen, Ngoc Phuoc Le, Viet Anh Dang, "*Dual-Observer based Framework for Fault-Tolerant Trajectory Tracking of Non-holonomic Wheeled Mobile Robots*", J Robot Control (JRC), vol. 6, no. 6, pp. 2871–2882, Dec. 2025. DOI: 10.18196/jrc.v6i6.28586 **(SCOPUS-Q2)**

[CT7]. Van Du Phan, The Anh Mai, **Sy Phuong Ho**, Thai Son Dang, Van Chuong Le, Van Nam Dinh. "*Development of an Adaptive Integral Terminal Sliding Mode Tracking Control for a Wheeled Mobile Robot With Time Delay Estimation*". *Int. J. Control Autom. Syst.* 23, 2399–2410 (2025). https://doi.org/10.1007/s12555-024-0747-x. **(SCIE-Q2)**

[CT8]. Sy Phuong Ho, Manh Tien Ngo*, Duy Tan Ngo, Van Du Phan, Dinh Tu Duong, Van Vy Phan, "*Hybrid Fault-Tolerant Adaptive Controller for Robust Trajectory Tracking of Mobile Robots"*, Transactions of the Institute of Measurement and Control, pp. 1-11, 2026. Doi: 10.1177/01423312261449864 **(SCIE-Q2)**

[CT9]. Sy Phuong Ho, Manh Tien Ngo*, Duy Tan Ngo, Van Du Phan, Thai Son Dang, Dinh Tu Duong, Van Nam Dinh, Van Manh Tran, "*Robust Fault-tolerant Control based on the integration of controllers for Non-holonomic Mobile Robots with Disturbance Observers"*, International Journal of Control, Automation, and Systems. https://doi.org/10.1007/s12555-026-00093-8 **(SCIE-Q2)**